

Non-aqueous phase liquid-contaminated soil remediation by ex situ dielectric barrier discharge plasma

C. A. Aggelopoulos · C. D. Tsakiroglou ·
S. Ognier · S. Cavadias

Received: 4 July 2013 / Revised: 5 October 2013 / Accepted: 14 December 2013 / Published online: 9 January 2014
© Islamic Azad University (IAU) 2013

Abstract Non-thermal dielectric barrier discharge plasma is examined as a method for the ex situ remediation of non-aqueous phase liquid (NAPL)-contaminated soils. A mixture of equal mass concentrations (w/w) of *n*-decane, *n*-dodecane and *n*-hexadecane was used as model NAPL. Two soil types differing with respect to the degree of micro-heterogeneity were artificially polluted by NAPL: a homogeneous silicate sand and a moderately heterogeneous loamy sand. The effect of soil heterogeneity, NAPL concentration and energy density on soil remediation efficiency was investigated by treating NAPL-polluted samples for various treatment times and three NAPL concentrations. The concentration and composition of the residual NAPL in soil were determined with NAPL extraction in dichloromethane and GC-FID analysis, while new oxidized products were identified with attenuated total reflection Fourier transform infrared spectroscopy (ATR-FTIR). The experimental results indicated that the overall NAPL removal efficiency increases rapidly in early times reaching a plateau at late times, where NAPL is removed almost completely. The overall NAPL removal efficiency decreases with its concentration increasing and soil heterogeneity strengthening. The removal efficiency of each NAPL compound is inversely proportional to the number

of carbon atoms and consistent with alkane volatility. A potential NAPL degradation mechanism is suggested by accounting for intermediates and final products as quantified by GC-FID and identified by ATR-FTIR.

Keywords Dielectric barrier discharge · Non-aqueous phase liquid removal efficiency · Plasma oxidation · Soil heterogeneity · Soil remediation

Introduction

The remediation of soils polluted by non-aqueous phase liquids (NAPLs) resulting from leaking storage tanks, spills and improper waste disposal is considered as one of the most significant challenges (Triplett Kingston et al. 2010). NAPLs have caused widespread subsurface contamination, while they tend to sink in groundwater systems, resulting in complex dispersal and plume patterns, which are long-term sources of subsurface pollution, and difficult to clean-up. In addition, the continuous dissolution of NAPLs may lead to the extensive contamination of groundwater. Soil remediation is commonly performed by technologies (e.g., thermal treatment, soil vapor extraction and bioremediation) based on the injection of steam, oxygen or remedial solutions, including permanganate, dithionate or nutrient amendments for bioremediation (Devlin and Barker 1994; Schnarr et al. 1998; Istok et al. 1999; Triplett Kingston et al. 2010). Aqueous solutions may be injected for the purposes of flushing or to promote the in situ degradation of contaminants (Barcelona and Xie 2001; Devlin et al. 2004). Most of the soil remediation technologies have a limited NAPL removal efficiency due to the retention of pollutants in low-permeability zones (e.g., soil vapor extraction) (Brusseau et al. 2010; Carroll et al. 2012) or are

C. A. Aggelopoulos (✉) · C. D. Tsakiroglou
Institute of Chemical Engineering Sciences, Foundation
for Research and Technology Hellas, Stadiou Str., Platani,
26504 Patras-Rio, Greece
e-mail: caggelop@iceht.forth.gr

C. A. Aggelopoulos · S. Ognier · S. Cavadias
Laboratoire de Génie des Procédés Plasmas et Traitements de
Surfaces - EA 3492, Université Pierre et Marie Curie – Ecole
Nationale Supérieure de Chimie de Paris, Pierre & Marie Curie
Str., 75231 Paris Cedex, France

applicable to source zones composed of volatile organic contaminants (e.g., air sparging, supersaturated water injection) (Nelson et al. 2009; Adams et al. 2011). Only incineration, smoldering combustion, bio-treatment and chemical oxidation may transform contaminants to less toxic or non-hazardous species (Gierczak et al. 2006; Switzer et al. 2009; Ko et al. 2012; Cai et al. 2012). Some of these methods are highly energy-consuming, and often a subsequent treatment of generated gases or liquids is required. Although the cost of soil remediation may be very different between different countries, some estimates are bioventing ~ 80 €/tn, soil vapor extraction ~ 100 €/tn, in situ thermal desorption ~ 100 – 150 €/tn, in situ oxidation ~ 100 – 150 €/tn, ex situ bioremediation ~ 100 €/tn and ex situ incineration cost ~ 500 – 1000 €/tn (Khan et al. 2004). Another problem of key importance is the potential transfer of a fraction of the pollutant mass from the subsurface toward the surrounding environment, i.e., air and groundwater. There is a lack of cost-effective technologies promoting the fast removal of organic pollutants from soils, avoiding their transfer to water or air and minimizing the environmental impacts.

During the last years, the non-thermal plasma discharge (NTP) has been considered as a well-promising advanced oxidation process (AOP) and is used as an energetically efficient method of wastewater treatment (Locke et al. 2006; Hao et al. 2007; Zhang et al. 2008; Ognier et al. 2009; Qu et al. 2009). Additionally, NTP has extensively been studied for the treatment of polluted gases and has been used successfully for the removal of various hydrocarbon pollutants such as aliphatics, aromatic compounds, aromatic polycyclic compounds and halogenated solvents (Masuda 1988; Mok et al. 2002; Kim 2003; Lee et al. 2004; Kim et al. 2005; Bai et al. 2009). NTP is unique in inducing various non-equilibrium chemical reactions at room temperature. During the discharge, high-energy electrons are formed (Redolfi et al. 2009) producing secondary electrons and highly reactive species (such as OH, H, O radicals and H_2O_2 , O_3) capable of oxidizing the pollutants (Chang and Lin 2005).

Recently, a limited number of studies have been published on the treatment of polluted soils by NTP technologies (Wang et al. 2010, 2011; Redolfi et al. 2010; Lou et al. 2012). An electrical discharge can be created in the contaminated soil by imposing a high electric potential between two electrodes. In particular, dielectric barrier discharge (DBD) has been used to remediate soils contaminated by kerosene and chloramphenicol (Redolfi et al. 2010; Wang et al. 2011), while low-temperature pulsed corona discharge plasma has been used for the degradation of pentachlorophenol and p-nitrophenol in contaminated soils (Wang et al. 2010; Lou et al. 2012). Up-to-date, a little attention has been paid on the scale-up of the plasma discharge techniques to large-scale systems with the

capacity to remediate soils under continuous feed conditions.

In the present work, an ex situ DBD plasma reactor that can easily be up-scaled to industrial scale was used to remediate soils polluted by a model NAPL composed of *n*-alkanes (*n*- C_{10} , *n*- C_{12} and *n*- C_{16}). The experiments were repeated at various treatment times for two soil types differing with respect to the degree of micro-heterogeneity and polluted with various NAPL concentrations. In this manner, the overall NAPL removal efficiency as well as the NAPL compound removal efficiency was correlated with soil heterogeneity, NAPL concentration and energy consumption. Finally, a potential NAPL degradation mechanism was proposed based on the intermediates and final products of the process.

Materials and methods

Materials

The model NAPL was a mixture of equal mass concentrations (w/w) of three *n*-alkanes having different carbon atoms (*n*-decane, *n*-dodecane and *n*-hexadecane). All NAPL compounds (purity > 95 %) were purchased from Merck.

Soils were artificially contaminated by NAPL by mixing soil samples with NAPL solutions in acetone. After mixing, the soil samples were placed into the fume hood until the acetone evaporation was completed. In this manner, soils contaminated by three different NAPL concentrations were obtained (1 g/kg-soil, 10 g/kg-soil, 100 g/kg-soil).

Two soil types differing with respect to the degree of micro-heterogeneity were polluted with the aforementioned NAPL: a homogeneous silicate sand with narrow grain size distribution and a loamy sandy soil collected from the region of Western Greece, with a broad grain size distribution (Table 1). The content of sand, silt and clay in loamy sand were 83, 4 and 13 %, respectively.

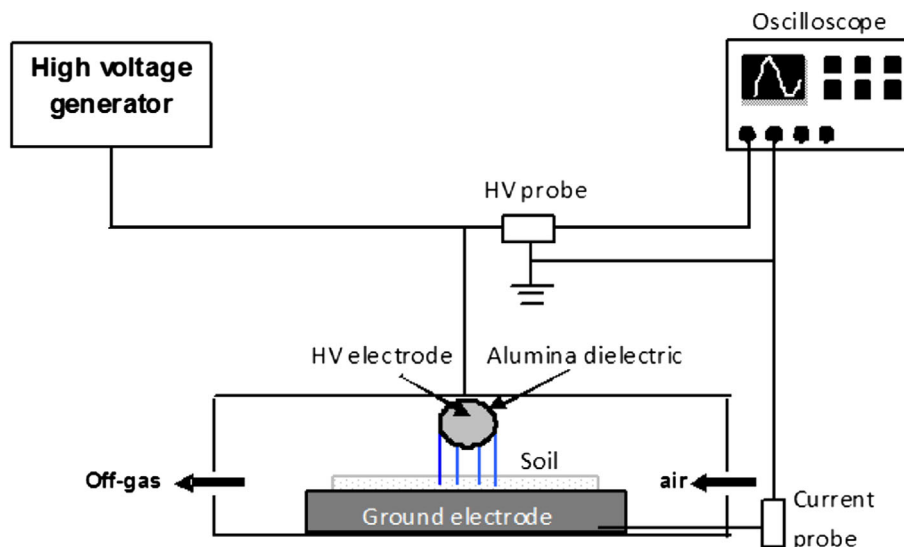
Experimental setup

The schematic diagram of the experimental apparatus used to perform ex situ DBD plasma experiments at atmospheric pressure is shown in Fig. 1. The apparatus consisted of a high-voltage generator supplying an alternative voltage ranging from 12 to 14 kV peak to peak with a constant frequency of 40 kHz and a cylinder-to-plane reactor inserted in a Plexiglas box. The voltage and current were measured with a digital oscilloscope (LeCroy LT 342, 500 MHz), and the plasma discharge power P was calculated by integrating the instantaneous voltage and current. The DBD reactor (Fig. 1) consisted of a stainless steel

Table 1 Soil properties

| Soil | Homogeneous sand | Loamy sandy soil |
|-------------------------|----------------------------------|---|
| Grain size distribution | Narrow (125–250 μm) | Broad ^a (<2 μm –2 mm) |
| Porosity, ϕ | 0.4 | 0.45 |
| Permeability, k | $25 \times 10^{-12} \text{ m}^2$ | $385 \times 10^{-15} \text{ m}^2$ |
| Formation factor, F | 3.5 | 4.7 |

^a $d_g > 125 \mu\text{m}$: 69 %; $50 \mu\text{m} < d_g < 125 \mu\text{m}$: 14 %; $2 \mu\text{m} < d_g < 50 \mu\text{m}$: 4 %; $d_g < 2 \mu\text{m}$: 13 %

Fig. 1 Experimental apparatus

high-voltage electrode covered by 4 mm thickness dielectric of alumina, and a stainless steel ground electrode. The high-voltage electrode had length and diameter equal to 80 and 13 mm, respectively, while the ground electrode was a belt conveyor of dimensions 97 mm \times 85 mm \times 10 mm moving with the aid of a motor in both directions at a constant velocity of 40 mm min^{-1} . The gap between the dielectric and ground electrode was fixed at 2 mm.

In each experiment, 5 g of contaminated soil was spread uniformly on the ground electrode at a thickness close to 1 mm. Atmospheric pressure air was injected at constant flow rate of 1 L min^{-1} . The soil treatment time was controlled by the number of passes of belt conveyor. Control experiments (ventilation without plasma discharge) were also performed. All experiments were conducted in duplicates with the standard deviation of experimental data being negligible.

Analytical techniques

After the completion of plasma treatment, the soil samples were immediately placed into PTFE cap glass flasks containing 5 ml of dichloromethane (DCM, Sigma-Aldrich), which is used as extraction solvent. All flasks were shaken for 2.5 h on an overhead shaker at a speed of 12 rpm, and

then, sodium sulfate (Na_2SO_4) was added to adsorb any water traces. The organic extracts were filtered through 0.45- μm PTFE filters with a glass syringe and transferred into a clear vial glass with a Teflon septum on the screw cap and stored at 4 $^\circ\text{C}$. Finally, the filtrates were used to analyze the residual NAPL in soil. Control experiments in untreated soil samples showed that the NAPL recovery from soil was greater than 99 %.

The concentration of NAPL compounds ($n\text{-C}_{10}$, $n\text{-C}_{12}$ and $n\text{-C}_{16}$) in the soil matrix was measured with gas chromatography–flame ionization detection (GC-FID). A Shimadzu GC-FID (GC 2014) equipped with a fused silica capillary column (50 m \times 0.2 mm i.d \times 0.5 μm film thickness, PETROCOL, Supelco) was used to separate and identify the NAPL compounds. High-purity helium was used as a carrier gas at a constant flow rate of 15.9 ml/min. The sample injection volume was 1 μL , and the split ratio was fixed at 1:15. The injector and detector temperature were set to 250 and 280 $^\circ\text{C}$, respectively. The oven temperature was kept at 40 $^\circ\text{C}$ for 10 min, ramped up at a rate of 1.1 $^\circ\text{C min}^{-1}$ to 114 $^\circ\text{C}$ and subsequently ramped up at a rate of 1.7 $^\circ\text{C min}^{-1}$ to 250 $^\circ\text{C}$ where it was kept constant for 15 min. The concentration of each NAPL compound was measured by constructing calibration curves of standard mixtures of $n\text{-C}_{10}$, $n\text{-C}_{12}$ and $n\text{-C}_{16}$.

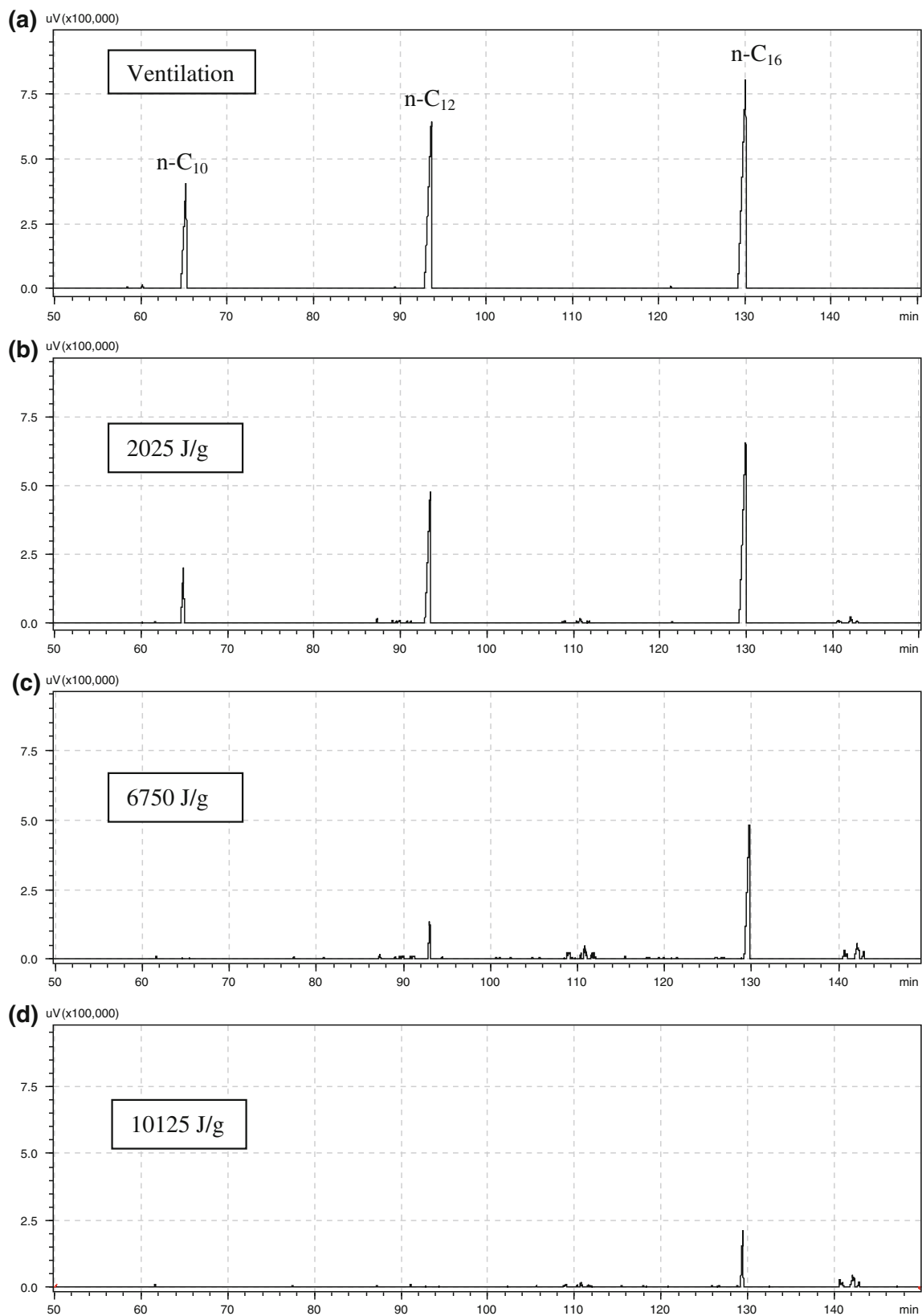


Fig. 2 GC-FID chromatograms of untreated and treated homogeneous sand extracts



In order to identify eventual intermediate products, some filtrates were analyzed by attenuated total reflection Fourier transform infrared spectroscopy (ATR-FTIR). ATR-FTIR is a non-destructive method, and solid or liquid samples can be analyzed without the necessity of any pre-treatment. All spectra were taken at a spectral resolution of 4 cm^{-1} with wavenumber ranging from 500 to 4000 cm^{-1} .

Results and discussion

NAPL remediation by DBD plasma treatment

Prior to DBD plasma treatment, control ventilation experiments were performed and it was found that after the treatment, the NAPL concentration in soil remained almost unaltered. Plasma discharge experiments were performed at various treatment times ranging from 2.5 to 33 min, corresponding to energy densities (E_D) from 675 to 10125 J/g soil. The energy density is defined as

$$E_D = Pt/m \quad (1)$$

where P is the calculated power of plasma discharge ($\sim 25\text{ W}$ in this study), t is the treatment time (s), and m is the mass of soil treated (g).

GC-FID chromatograms obtained from the analysis of the extracts of NAPL-contaminated homogeneous sand after 33 min of ventilation and after the plasma discharge treatment for various times (corresponding to energies 2025, 6750 and 10125 J/g) are shown in Fig. 2. The three NAPL compounds ($n\text{-C}_{10}$, $n\text{-C}_{12}$ and $n\text{-C}_{16}$) were clearly identified from the peaks at retention time 65, 93 and 129 min, respectively. Though initially all NAPL compounds are contained in soil at the same concentration, the height of the peak increases as the number of carbon atoms increases (Fig. 2a). All alkanes were gradually degraded as the injected energy increased, and this is reflected in the decrease in the height of the peaks as compared to the corresponding ones of the untreated sample (Fig. 2). On the other hand, as the volatility of the compound increases, its removal accelerates (Fig. 2). At the highest energy density, neither $n\text{-C}_{10}$ nor $n\text{-C}_{12}$ was detected, while a small amount of $n\text{-C}_{16}$ was still detectable (Fig. 2d).

Effects of energy density and NAPL concentration on NAPL remediation

The NAPL removal efficiency as a function of energy density for various initial NAPL concentrations is shown in Fig. 3. The NAPL removal efficiency was an increasing function of energy density, which is similar to that reported

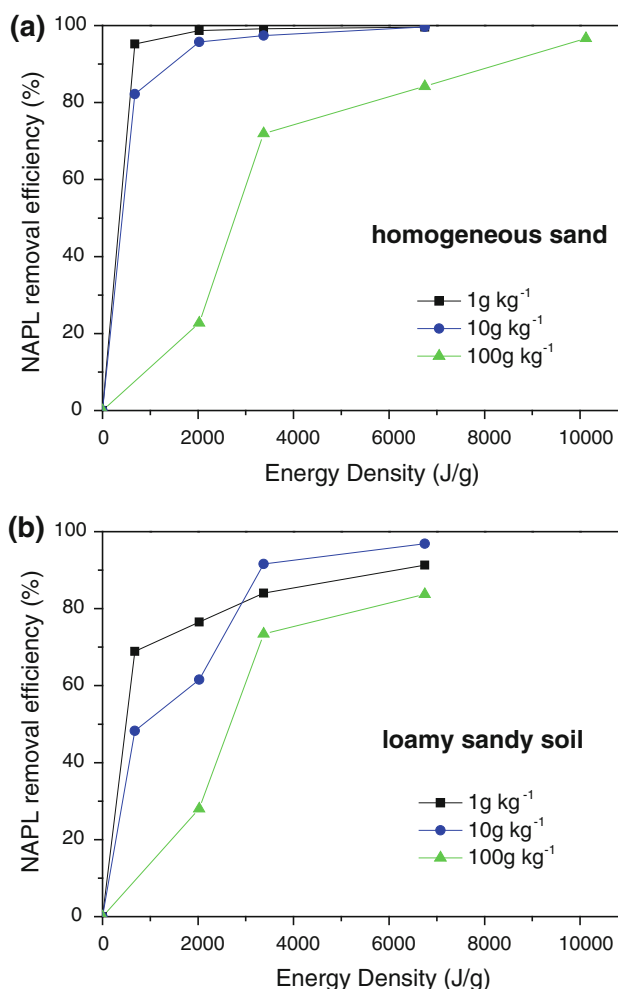


Fig. 3 Effect of NAPL concentration on NAPL removal efficiency **a** homogeneous sand; **b** loamy sandy soil

in the literature (Wang et al. 2010, 2011; Lou et al. 2012). At lower energy densities, the NAPL removal efficiency increased rapidly, while at higher energy densities, the NAPL removal efficiency increased slowly tending asymptotically to stabilize (Fig. 3). At early treatment times (low energy density), where NAPL concentration in soil is high, the produced plasma species come in contact very fast with NAPL molecules and the reaction is fast. At late treatment times (high energy density), where NAPL molecules have been sufficiently removed, plasma species do not collide with NAPL molecules so frequently and the reaction becomes slow.

For the homogeneous sand and NAPL concentrations $1\text{--}10\text{ g kg}^{-1}$, the NAPL removal efficiency was maximized ($\sim 100\%$) at very low energy density corresponding to short period of soil treatment (Fig. 3a). At high initial NAPL concentrations (100 g kg^{-1}), the NAPL removal efficiency became respectable at a high energy density ($\sim 10000\text{ J/g}$) (Fig. 3a). For the loamy sandy soil, the

NAPL remediation efficiency reached $\sim 84\%$ for the highest NAPL concentration (100 g kg^{-1}) and maximum energy density of 6750 J/g , whereas the NAPL remediation

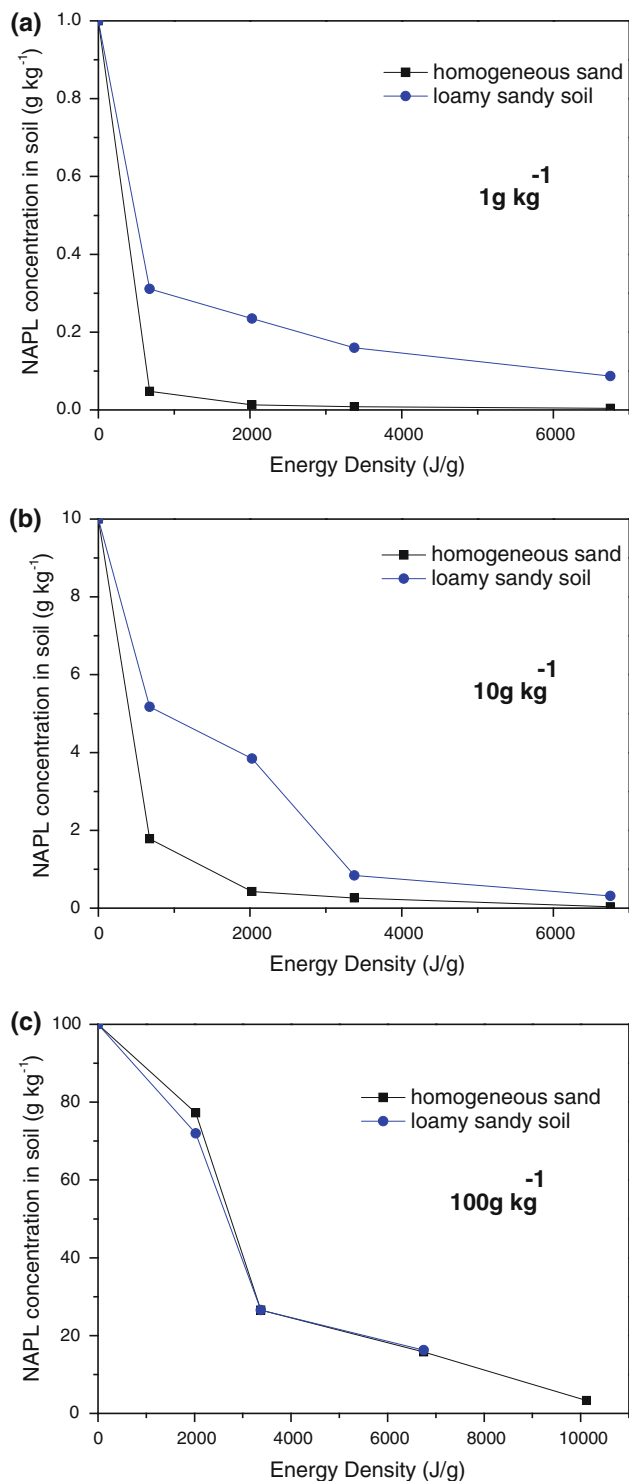


Fig. 4 Effect of soil heterogeneity on NAPL concentration in soil for various initial NAPL concentrations **a** 1 g kg^{-1} ; **b** 10 g kg^{-1} ; **c** 100 g kg^{-1}

rate (as it is quantified by the slope of the curve) was finite (Fig. 3b). At concentrations $1\text{--}10\text{ g kg}^{-1}$, the NAPL removal efficiency ranges from 92 to 97 %, but still has the tendency to increase with energy density (Fig. 3b). Therefore, we could suppose that NAPL removal efficiency might approach, also, to 100 % at very high energy densities ($>10000\text{ J/g}$).

Effect of soil heterogeneity on NAPL remediation

For an initial NAPL concentration equal to 1 g kg^{-1} (Fig. 4a), the NAPL concentration was decreased more rapidly for the homogeneous sand compared to the moderately heterogeneous loamy sandy soil. At energy density of 6750 J/g , corresponding to 24.5 min of plasma treatment time, the residual NAPL mass in homogeneous sand and loamy sand was 4 and 80 mg, respectively. Likewise, for initial NAPL concentration equal to 10 g kg^{-1} (Fig. 4b), the residual NAPL mass after 24.5 min of plasma treatment was 37 and 310 mg, respectively. In other words, for initial NAPL concentrations of $1\text{--}10\text{ g kg}^{-1}$, the NAPL removal efficiency was lower for the loamy sand compared to the homogeneous sand, at a given energy density. For initial NAPL concentration of 100 g kg^{-1} (Fig. 4c), where 60 % of soil porosity is saturated by NAPL, the decrease in NAPL concentration was almost identical for both soils and insensitive to heterogeneity.

In general, due to soil hydrophilicity and capillary forces, NAPL blobs prefer to occupy the larger pores than the smaller ones. At low NAPL saturation, the air, flowing in parallel to the soil layer and above it, is accessible to NAPL blobs, and the “in-plane” NAPL removal in homogeneous sand is expected to proceed uniformly in accordance with the narrow pore size distribution and uniform sizes of NAPL blobs. In contrast, in loamy sandy soil, the smaller

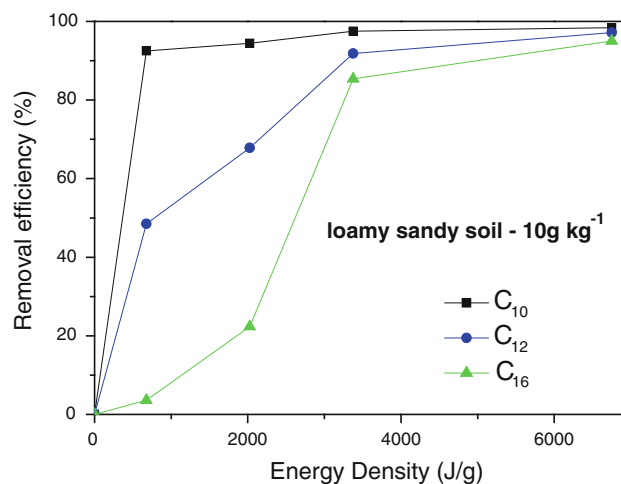


Fig. 5 Removal efficiency of each NAPL compound



Fig. 6 FTIR spectra of NAPL-contaminated homogeneous sand (100 g Kg⁻¹) extracts before and after plasma treatment

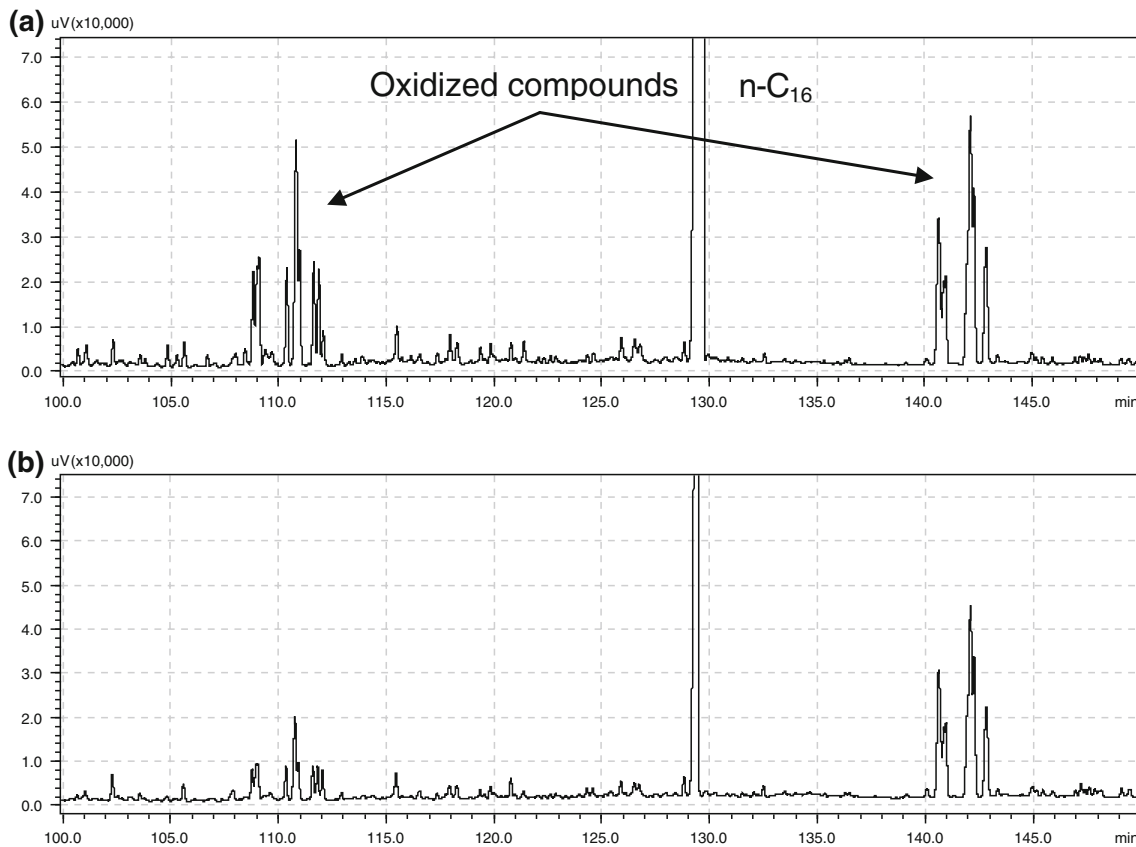
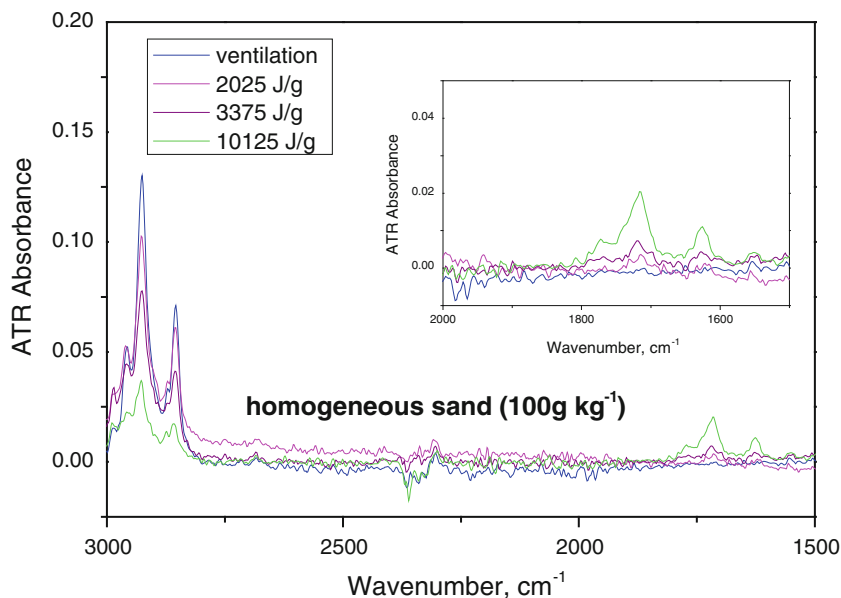
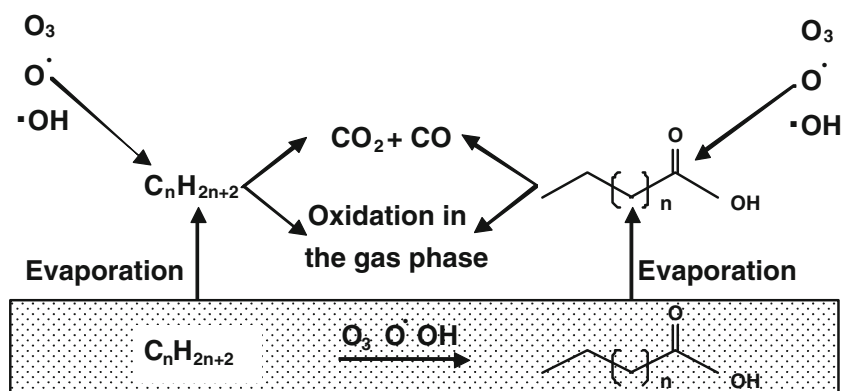


Fig. 7 GC-FID chromatograms of homogeneous sand extracts at energy density **a** 6750 and **b** 10125 J/g

air/NAPL interfacial area of large NAPL-occupied pores may lead to weaker “in-plane” NAPL removal rate and subsequently to lower NAPL removal efficiency. At high

NAPL saturation, in both soils, the majority of the pore space is occupied by NAPL, except of very small pores, and initially, the in-plane air/NAPL interfacial area,

Fig. 8 NAPL removal mechanism



available for “in-plane” removal, is limited. Under such conditions, the air overlying the soil favors the through-plane (a vertical layer-by layer) removal of NAPL, which is expected to be slow and independent of soil heterogeneity.

Removal efficiency of each NAPL compound

The overall NAPL removal efficiency is controlled by the individual removal efficiency of each component (n -C₁₀, n -C₁₂ and n -C₁₆). The remediation efficiency of each NAPL compound as a function of energy density is shown in Fig. 5. It is evident that the energy density (treatment time) required to remove NAPL compounds follows the sequence n -C₁₆ > n -C₁₂ > n -C₁₀. In other words, the time needed to remediate alkanes is proportional to the number of carbon atoms (in agreement with the energy requirements of the corresponding oxidation reactions) and inversely proportional to their volatility. For high energy densities (~ 10000 J/g), the remediation efficiency has the tendency to stabilize regardless of carbon atoms (Fig. 5).

NAPL degradation mechanism

ATR-FTIR measurements performed on extracts taken from the homogeneous sand (100 g kg^{-1}) are shown in Fig. 6. During DBD plasma treatment, the three peaks corresponding to C–H group (CH, CH₂ and CH₃ at 2855, 2925 and 2956 cm^{-1} , respectively) gradually weaken because of the NAPL removal. At high energy density, two new peaks were detected at 1630 and 1720 cm^{-1} (Fig. 6). The peak at 1720 cm^{-1} is assigned to carboxylic group, while the peak at 1630 cm^{-1} is assigned to C = C groups (Coates 2000). Obviously, these new compounds were products of the direct oxidation of NAPL in the soil, at energy density higher than 3375 J/g, where the removal efficiency of n -C₁₀, n -C₁₂ and n -C₁₆ was about 90, 30 and

10 %, respectively. One of the main features of non-thermal plasma is that locally and across the plasma discharge, the temperature may reach to several hundred of Celsius degrees, and such high temperatures may stimulate the evaporation of pollutants. We suppose that for the most volatile compounds (n -C₁₀), their removal is favored due to the enhanced evaporation followed by the alkane oxidation in the gas phase. On the other hand, NAPL oxidation in soil matrix occurs only for the heavier and less volatile compounds (n -C₁₂ and n -C₁₆). To quantify the oxidized products detected by FTIR, a semi-quantitative approach was used (Redolfi et al. 2010) based on the new peaks detected with GC-FID at retention time of ~ 110 and ~ 140 min (Fig. 7). The carbon content in the oxidized compounds was found to be ~ 15 % of the carbon content in the initial n -C₁₂ and n -C₁₆, at energy density of 6750 J/g (Fig. 7a). Nevertheless, at energy density of 10125 J/g, these oxidized compounds have been partially removed and only 5 % of the initial carbon content of n -C₁₂ and n -C₁₆ remained in the soil (Fig. 7b). Therefore, even for the heavier NAPL molecules, it seems that the main removal mechanism is the evaporation followed by oxidation in the gas phase. Based on these results, a possible NAPL removal mechanism is suggested in Fig. 8. However, in order to confirm this assumption, a detailed analysis of the exhaust gases (Sivachandiran et al. 2013) is required.

Conclusion

Ex situ DBD plasma discharge experiments were performed in NAPL-contaminated soils to evaluate the remediation efficiency as a function of soil heterogeneity, NAPL concentration and composition, and energy consumption. At low energy densities, NAPL remediation efficiency decreases as NAPL concentration increases and soil heterogeneity is enhanced. At high NAPL

concentrations, the remediation efficiency becomes independent of soil heterogeneity. At high energy densities (~ 10000 J/g-soil), NAPL is completely removed, indicating that all NAPL compounds (n -C₁₀, n -C₁₂ and n -C₁₆) are oxidized, regardless of NAPL concentration and soil heterogeneity. At a given energy density, the removal efficiency decreases as the number of carbon atoms increases in agreement with their volatility and energy required for their oxidation. Based on the intermediate and final products identified in soil, a mechanism of remediation is suggested where the most volatile NAPL compounds are evaporated and then oxidized in gas phase, whereas the less volatile compounds are evaporated and oxidized in gas phase and soil matrix.

Acknowledgments This research has been co-financed by the European Union (European Social Fund–ESF) and Greek National Funds through the Operational Program “Education and Lifelong Learning” of the National Strategic Reference Framework (NSRF)—Research Funding Program: Supporting Postdoctoral Researchers.

References

- Adams JA, Reddy KR, Tekola L (2011) Remediation of chlorinated solvents plumes using in situ air sparging-A 2-D laboratory study. *Int J Environ Res Public Health* 8:2226–2239
- Bai HY, Chen JR, Li XY, Zhang CH (2009) Non-thermal plasmas chemistry as a tool for environmental pollutants abatement. *Rev Environ Contam Toxicol* 201:117–136
- Barcelona MJ, Xie G (2001) In situ lifetimes and kinetics of a reductive whey barrier and an oxidative ORC barrier in the subsurface. *Environ Sci Technol* 35:3378–3385
- Brusseau ML, Rohay V, Truex MJ (2010) Analysis of soil vapor extraction data to evaluate mass-transfer constraints and estimate source-zone mass flux. *Ground Water Monit Remediat* 30:57–64
- Cai XD, Du WT, Wu JY, Li RF, Guo Y, Yang ZJ (2012) Effective treatment of trichloroethylene-contaminated soil by hydrogen peroxide in soil slurries. *Pedosphere* 22:572–579
- Carroll KC, Oostrom M, Truex MJ, Rohay VJ, Brusseau ML (2012) Assessing performance and closure for soil vapor extraction: integrating vapor discharge and impact to groundwater quality. *J Contam Hydrol* 128:71–82
- Chang CL, Lin TS (2005) Decomposition of toluene and acetone in packed dielectric barrier discharge reactors. *Plasma Chem Plasma Process* 25:641–657
- Coates J (2000) Interpretation of infrared spectra, a practical approach. In: Meyers RA (ed) *Encyclopedia of analytical chemistry*. Wiley, Chichester, pp 10815–10837
- Devlin JF, Barker JF (1994) A semipassive nutrient injection scheme for enhanced in situ bioremediation. *Ground Water* 32:374–380
- Devlin JF, Katic D, Barker JF (2004) In situ sequenced bioremediation of mixed contaminants in groundwater. *J Contam Hydrol* 69:233–261
- Gierczak RFD, Devlin JF, Rudolph DL (2006) Combined use of field and laboratory testing to predict preferred flow paths in an heterogeneous aquifer. *J Contam Hydrol* 82:75–98
- Hao XL, Zhou MH, Lei LC (2007) Non-thermal plasma-induced photocatalytic degradation of 4-chlorophenol in water. *J Hazard Mater* 141:475–482
- Istok JD, Amonette JE, Coe CR, Fruchter JS, Humphrey MD, Szczyty JE, Teel SS, Vermeul VR, Williams MD, Yabusaki SB (1999) In situ redox manipulation by dithionite injection: intermediate-scale laboratory experiments. *Ground Water* 37:884–889
- Khan FI, Husain T, Hejazi R (2004) An overview and analysis of site remediation technologies. *J Environ Manag* 71:95–122
- Kim HH (2003) Plasma-driven catalyst processing packed with photocatalyst for gas-phase benzene decomposition. *Catal Commun* 4:347–351
- Kim HH, Ogata A, Futamura S (2005) Atmospheric plasma-driven catalysis for the low temperature decomposition of dilute aromatic compounds. *J Phys D Appl Phys* 38:1292–1299
- Ko S, Crimi M, Marvin BK, Holmes V, Huling SG (2012) Comparative study on oxidative treatments of NAPL containing chlorinated ethanes and ethenes using hydrogen peroxide and persulfate in soils. *J Environ Manag* 108:42–48
- Lee BY, Park SH, Lee SC, Kang M, Choung SJ (2004) Decomposition of benzene by using a discharge plasma-photocatalyst hybrid system. *Catal Today* 93–95:769–776
- Locke BR, Sato M, Sunka P, Hoffman MR (2006) Electrohydraulic discharge and nonthermal plasma for water treatment. *Ind Eng Chem Res* 45:882–905
- Lou J, Lu N, Li J, Wang T, Wu Y (2012) Remediation of chloramphenicol-contaminated soil by atmospheric pressure dielectric barrier discharge. *Chem Eng J* 180:99–105
- Masuda S (1988) Pulsed corona induced plasma chemical process: a horizon of new plasma chemical technologies. *Pure Appl Chem* 60:727–731
- Mok YS, Nam CM, Cho MH, Nam IS (2002) Decomposition of volatile organic compounds and nitric oxide by nonthermal plasma discharge processes. *IEEE Trans Plasma Sci* 30:408–416
- Nelson L, Barker J, Li T, Thomson N, Ioannidis M, Chatzis J (2009) A field trial to assess the performance of CO₂-supersaturated water injection for residual volatile LNAPL recovery. *J Contam Hydrol* 109:82–90
- Ognier S, Iya-Sou D, Fourmond C, Cavadias S (2009) Analysis of mechanisms at the plasma-liquid interface in a gas-liquid discharge reactor used for treatment of polluted water. *Plasma Chem Plasma Process* 29:261–273
- Qu GZ, Lu N, Li J, Wu Y, Li GF, Li D (2009) Simultaneous pentachlorophenol decomposition and granular activated carbon regeneration assisted by dielectric barrier discharge plasma. *J Hazard Mater* 172:472–478
- Redolfi M, Aggadi N, Duten X, Touchard S, Pasquiers S, Hassouni K (2009) Oxidation of acetylene in atmospheric pressure pulsed corona discharge cell working in the nanosecond regime. *Plasma Chem Plasma Process* 29:173–195
- Redolfi M, Makhloufi C, Ognier S, Cavadias S (2010) Oxidation of kerosene components in a soil matrix by a dielectric barrier discharge reactor. *Process Saf Environ Prot* 88:207–212
- Schnarr M, Truax C, Farquhar G, Hood E, Gonullu T, Stickney B (1998) Laboratory and controlled field experiments using potassium permanganate to remediate trichloroethylene and perchloroethylene DNAPLs in porous media. *J Contam Hydrol* 29:205–224
- Sivachandiran L, Thevenet F, Gravejat P, Rousseau A (2013) Isopropanol saturated TiO₂ surface regeneration by non-thermal plasma: influence of air relative humidity. *Chem Eng J* 214:17–26
- Switzer C, Pironi P, Gerhard JI, Rein G, Torero JL (2009) Self-sustaining smoldering combustion: a novel remediation process for non-aqueous-phase liquids in porous media. *Environ Sci Technol* 43:5871–5877
- Triplett Kingston JL, Dahlen PR, Johnson PC (2010) State-of-the-practice review of in situ thermal technologies. *Ground Water Monit Remediat* 30:64–72



- Wang TC, Lu N, Li J, Wu Y (2010) Degradation of pentachlorophenol in soil by pulsed corona discharge plasma. *J Hazard Mater* 180:436–441
- Wang TC, Lu N, Li J, Wu Y (2011) Plasma-TiO₂ catalytic method for high-efficiency remediation of p-Nitrophenol contaminated soil in pulsed corona. *Environ Sci Technol* 45:9301–9307
- Zhang Y, Zheng J, Qu X, Yu W, Chen H (2008) Catalytic effect of activated carbon and activated carbon fiber in non-equilibrium plasma-based water treatment. *Plasma Sci Technol* 10:358–362

